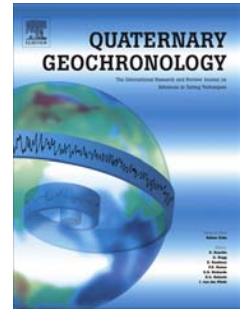


Accepted Manuscript

Combining surface exposure dating and burial dating from paired cosmogenic depth profiles. Example of El Límite alluvial fan in Huércal-Overa basin (SE Iberia)

Angel Rod´es, Raimon Pall`as, Mar´ia Ortu˜no, Eduardo Garc´ia-Melendez, Eul`alia Masana



PII: S1871-1014(13)00092-7

DOI: [10.1016/j.quageo.2013.10.002](https://doi.org/10.1016/j.quageo.2013.10.002)

Reference: QUAGEO 545

To appear in: *Quaternary Geochronology*

Received Date: 29 February 2012

Revised Date: 1 October 2013

Accepted Date: 3 October 2013

Please cite this article as: Rod´es, A., Pall`as, R., Ortu˜no, M.´i., Garc´ia-Melendez, E., Masana, E.´a., Combining surface exposure dating and burial dating from paired cosmogenic depth profiles. Example of El Límite alluvial fan in Huércal-Overa basin (SE Iberia), *Quaternary Geochronology* (2013), doi: 10.1016/j.quageo.2013.10.002.

This is a PDF file of an unedited manuscript that has been accepted for publication. As a service to our customers we are providing this early version of the manuscript. The manuscript will undergo copyediting, typesetting, and review of the resulting proof before it is published in its final form. Please note that during the production process errors may be discovered which could affect the content, and all legal disclaimers that apply to the journal pertain.

Combined surface exposure and burial dating provides robust minimum and maximum ages. It also provides constraints for the exhumation rate and sediment residence time. Results suggest that El Límite alluvial fan was deposited in the Late Pleistocene. El Límite sediments were reworked due to the activity of the South-AMF.

ACCEPTED MANUSCRIPT

Combining surface exposure dating and burial
dating from paired cosmogenic depth profiles.
Example of El Límite alluvial fan in
Huércal-Overa basin (SE Iberia)

Several authors*

October 1, 2013

Abstract

Cosmogenic nuclide depth-profiles are used to calculate the age of landforms, the rates at which erosion has affected them since their formation and, in case of deposits, the paleo-erosion rate in the source area. However, two difficulties are typically encountered: 1) old deposits or strongly affected by cosmogenic nuclide inheritance often appear to be saturated, and 2) a full propagation of uncertainties often yields poorly constrained ages. Here we show how to combine surface-exposure-dating and burial-dating techniques in the same profile to get more accurate age results and to constrain the extent of pre-depositional burial periods. A ^{10}Be - ^{26}Al depth-profile measured in an alluvial fan of SE Iberia is presented as a natural example.

Keywords: Cosmogenic dating, Quaternary, Geomorphology, Numerical model, Eastern Betics

Ángel Rodés (,1,2), Raimon Pallàs (2), María Ortuño (2), Eduardo García-Melendez (3), Eulàlia Masana (2) (*) angelrodes@gmail.com (1) CIAF, Scottish Universities Environmental Research Centre, East Kilbride G75 0QF, United Kingdom (2) RISKNAT, Facultat de Geologia, Universitat de Barcelona, Martí i Franquès s/n, 08028 Barcelona, Spain (3) Área de Geodinámica Externa, Facultad de Ciencias Ambientales, Universidad de León, Campus de Vegazana s/n, 24071 León, Spain

1 Introduction

Cosmogenic exposure dating is a dependable technique in landscape evolution studies, as it can be used to deduce the exposure age of a landform surface (Gosse and Phillips, 2001). The concentration of cosmogenic nuclides in near-surface sediments depends, among other parameters, on the initial cosmogenic signature (i.e. initial concentrations), the erosion rate of the surface, and on the time of exposure to cosmic radiation. These parameters can be deduced from depth-profile datasets by inverse modeling (e.g. Anderson et al., 1996; Hancock et al., 1999; Siame et al., 2004; Braucher et al., 2009; Nissen et al., 2009; Hidy et al., 2010). However, when the landform under study is old compared to the cosmogenic nuclide half-life, or when the surface is affected by fast erosion processes, the age of the landform may not be constrained using this approach (see examples of "saturated" depth-profiles in Siame et al., 2004). Moreover, ages calculated by fitting the cosmogenic exposure model (Lal, 1991) can be very sensitive to variations of other poorly known parameters, such as the variations in the density of the sediments (Rodés et al., 2011) or the production of cosmogenic nuclides due to neutron and muon radiation (Braucher et al., 2011).

Cosmogenic burial dating is a technique based on the well known radioactive decay rates of cosmogenic nuclides, and is widely used in many areas of the Earth sciences and archeology (Granger and Smith, 2000). Dating materials by radioactive decay of cosmogenic nuclides requires that the sample has been completely shielded (deep burial) from cosmic radiation after the first exposure phase (e.g. Granger and Muzikar, 2001; Balco and Rovey, 2008). This simple exposure-burial history is difficult to assume in alluvial sediments, as they may be reworked from older landforms. Moreover, most of alluvial sediments are rarely buried at great depths.

In this work, we present a model that combines both cosmogenic nuclide exposure and burial models of near-surface sediments. Similar approaches have been described by Wolkowinsky and Granger (2004) and Mercader et al. (2012). However, the model presented here considers the possibility of a complex exposure-burial history of the sediments before their deposition. We test the benefits of the model by comparing the results of the combined surface exposure-burial (CSEB) model and the results of surface exposure model when fitting a c. 3 m depth-profile dataset from SE Iberia (Fig. 1).

2 Modeling ^{10}Be - ^{26}Al depth-profiles

To numerically estimate the age and the erosion rate experienced at a depositional landform surface, Siame et al. (2004), Hidy et al. (2010), Braucher et al. (2009) and Rodés et al. (2011) used the chi-square inverse approach to fit synthetic cosmogenic depth-profile models to measured datasets. In this work, we follow the approach of Rodés et al. (2011) but we use a combined surface exposure-burial (CSEB) model to take advantage of paired cosmogenic nuclide depth profiles.

2.1 Surface exposure model

The cosmogenic nuclide concentration (E) accumulated at a depth x (g cm^{-2}) from the top surface of a deposit, which has been eroding at a constant rate ε ($\text{g cm}^{-2} \text{ a}^{-1}$) since its formation (t years ago), was described by Lal (1991) and can be expressed as:

$$E_{(x,\varepsilon,t)} = \frac{P_{spal.}}{\frac{\varepsilon}{\Lambda_{spal.}} + \lambda} e^{-\frac{x}{\Lambda_{spal.}}} \left(1 - e^{-t\left(\lambda + \frac{\varepsilon}{\Lambda_{spal.}}\right)} \right) + \frac{P_{stop}}{\frac{\varepsilon}{\Lambda_{stop}} + \lambda} e^{-\frac{x}{\Lambda_{stop}}} \left(1 - e^{-t\left(\lambda + \frac{\varepsilon}{\Lambda_{stop}}\right)} \right) + \frac{P_{fast}}{\frac{\varepsilon}{\Lambda_{fast}} + \lambda} e^{-\frac{x}{\Lambda_{fast}}} \left(1 - e^{-t\left(\lambda + \frac{\varepsilon}{\Lambda_{fast}}\right)} \right) \quad (1)$$

where $P_{spal.}$, P_{stop} and P_{fast} are the surface production rates due to spallation, stopping muons and fast muons in atoms $\text{g}^{-1} \text{ a}^{-1}$, which can be calculated using the CRONUS-Earth online calculator (Balco et al., 2008), $\Lambda_{spal.}$, Λ_{stop} and Λ_{fast} are the attenuation lengths of each process (g cm^{-2}), and λ is the isotope decay constant (a^{-1}). Granger and Muzikar (2001) used 3 exponential curves to fit muon production rates. However, 2 exponential curves yield a good fit at near surface conditions (Heisinger et al., 2002a,b; Balco et al., 2013). Depth can also be expressed as $x = \rho \cdot z$, where z is the current profile depth in cm and ρ is the mean density of the rock or sediment in g cm^{-3} .

Especially in the case of sediments, the cosmogenic nuclides accumulated in situ may add to the decayed initial concentration at time of deposition, commonly referred to as inheritance:

$$C_{Inher.}(C_{(x,0),t}) = C_{(x,0)} \cdot e^{-\lambda t} \quad (2)$$

Thus, the exposure model of a depth profile can be expressed as:

$$C_{(C(x,0),x,\varepsilon,t)} = C_{Inher.(C(x,0),t)} + E_{(x,\varepsilon,t)} \quad (3)$$

Assuming that the inheritance is statistically constant in a single deposit (amalgamated pebble or sand samples), this model allows to calculate the exposure age of a surface by measuring the cosmogenic nuclide concentrations of a set of samples from the same depth profile.

2.2 Burial model

Based on eq. 1, the cosmogenic nuclide concentration at the top surface of a rock surface continuously exhumed at a constant rate ε_r is:

$$C_{(\varepsilon_r)} = \frac{P_{spal.}}{\frac{\varepsilon_r}{\Lambda_{spal.}} + \lambda} + \frac{P_{stop}}{\frac{\varepsilon_r}{\Lambda_{stop}} + \lambda} + \frac{P_{fast}}{\frac{\varepsilon_r}{\Lambda_{fast}} + \lambda} \quad (4)$$

where $P_{spal.}$, P_{stop} and P_{fast} are the mean surface production rates at the exhumed area. If the exhumed material is deeply buried (negligible cosmic radiation) right after its erosion, the cosmogenic nuclide concentration $B_{(\varepsilon_r,t_b)}$ will decrease with time (t_b) according to its radioactive decay:

$$B_{(\varepsilon_r,t_b)} = C_{(\varepsilon_r)} \cdot e^{-\lambda t_b} \quad (5)$$

This model allows to calculate apparent burial ages by measuring two cosmogenic nuclides with different radioactive decay rates in the same buried sample. However, a simple erosion-burial history needs to be assumed to consider that the apparent burial age is the age of the deposit. As evidence supporting this assumption is generally lacking, in most natural cases apparent burial ages must be considered as representing maximum deposition ages of landforms under study.

2.3 Combined surface exposure - burial (CSEB) model

In a paired isotope banana plot (e.g. Bierman et al., 1999, Fig. 2), the burial model generates all natural cosmogenic signatures below the erosion equilibrium line. These ^{10}Be - ^{26}Al concentrations are the possible values that represent the history of any sediment in a basin dominated by denudation processes (Fig. 2). In the case of alluvial deposits deposited in a short period

of time, we can assume that the initial bulk cosmogenic signature of their sediments ($C_{(x,0)}$ in eq. 2) is well represented by the burial model. This allow us to suggest a combined cosmogenic concentration surface exposure and burial model as a function of:

- Apparent pre-deposition exhumation rate (ε_r in eqs. 4 and 5)
- Apparent pre-deposition burial time (t_b in eq. 5)
- Erosion rate (ε in eqs. 1 and 3)
- Age (t in eqs. 1, 2 and 3)

Thus, based on eqs. 1, 2, 3, 4 and 5, the CSEB model can be expressed as:

$$C_{(\varepsilon_r, t_b, \varepsilon, t)} = B_{(\varepsilon_r, t_b)} \cdot e^{-\lambda t} + E_{(x, \varepsilon, t)} \quad (6)$$

Assuming that pre-deposition history of the sediments can be complex, involving several exposure and burial phases, ε_r should be considered as a minimum value of the original exhumation rate, and t_b should be considered a minimum value for the residence time of the sediments between exhumation and last deposition.

2.4 χ^2 fit modeling

Following Rodés et al. (2011), we built a χ^2 function based on the model in eq. 3 or eq. 6 and two cosmogenic nuclides, such as ^{10}Be and ^{26}Al ,

$$\chi_{(\varepsilon_r, t_b, \varepsilon, t)}^2 = \sum_{i=0}^N \left[\left(\frac{C_i^{10\text{Be}} - C_{(\varepsilon_r, t_b, \varepsilon, t)}^{10\text{Be}}}{\sigma_{i(\varepsilon, t)}^{10\text{Be}}} \right)^2 + \left(\frac{C_i^{26\text{Al}} - C_{(\varepsilon_r, t_b, \varepsilon, t)}^{26\text{Al}}}{\sigma_{i(\varepsilon, t)}^{26\text{Al}}} \right)^2 \right] \quad (7)$$

where $C_i^{10\text{Be}}$ and $C_i^{26\text{Al}}$ are the measured concentrations from the N samples at x_i depths, $C_{(\varepsilon_r, t_b, \varepsilon, t)}^{10\text{Be}}$ and $C_{(\varepsilon_r, t_b, \varepsilon, t)}^{26\text{Al}}$ are the concentrations predicted by the model for each isotope, and $\sigma_{i(\varepsilon, t)}^{10\text{Be}}$ and $\sigma_{i(\varepsilon, t)}^{26\text{Al}}$ are the errors due to depth, density and analytical uncertainties, explained in Rodés et al. (2011).

2.5 Uncertainties of the results

Different approaches have been used to calculate the uncertainties of the free parameters of depth-profile models: (1) Monte Carlo simulations are used to calculate the χ^2 values of models that fit the data within a certain confidence level by assigning random values to the free parameters (e.g. Hidy et al., 2010). This method also allows to randomize all the input values (concentrations, production rates, depth, etc.) to propagate their uncertainties to the results. The frequencies of the free parameters that pass the χ^2 test are considered as probability distributions of the results. Moreover, Monte Carlo simulations do not require iterative calculations to minimize the χ^2 function and they can be performed very fast. (2) χ^2 minimization method is based in the use of iterative approaches to get the most probable values of the free parameters. It is slower and usually requires a manual approximation to start iterating. Moreover, usually the maximum number of iterations are limited in the standard minimization methods, and the computer often yields overflow errors when the starting parameters are not appropriate. However, it can provide exact probability distributions of the resulting free parameters (e.g. Rodés et al., 2011). Most of computing software programs currently used to deal with depth-profile models provide methods to minimize the χ^2 function for several free parameters (e.g. `fmincon` in MATLAB[®] and `Octave`^(GPL); `FindMinimum` in Mathematica[®]).

When the distribution of the solutions is well delimited in the free parameters space, both approaches provide similar results (e.g. Balco et al., 2011). However, using depth-profile models, these distributions are often dispersed in long and narrow χ^2 "valleys" (e.g. erosion rate *vs.* exposure time graphs in Siame et al., 2004). To ensure that these "valleys" are represented by a set of solutions using Monte-Carlo simulations, the main distance between simulated models in the parameters space must be much smaller than the width of the "valleys". These peculiarities of the χ^2 function may make it difficult to justify the constrains and the number of tests in a Monte Carlo simulation in order to demonstrate, not only that the simulation results fit the data, but also that other results do not fit the data.

In this work, we have used a method that profits from both approaches. It randomizes 10000 combinations of the free parameters in a wide window (e.g. ages between 0 and 10Ma), selects the best 100 χ^2 results, use them as starting points for the χ^2 minimizations, and select the best result. Positive free parameters were the only constraints imposed to the models in the

χ^2 minimization. This method is relatively fast, allows to discard the few overflow errors obtained, and provides exact probability distributions of the parameters with no geological constraint.

3 Field example: El Límite alluvial fan, Huércal-Overa basin

The Huércal-Overa Basin is one of a series of Neogene and Quaternary sedimentary basins located within the Betic Cordillera of south-east Spain. The Plio-Quaternary deformation of the Huércal-Overa Basin is associated with left-lateral strike-slip and reverse faulting in relation to its position within the Eastern Betic Shear Zone, resulting in the development of a series of progressive unconformities, angular unconformities and faulting within the alluvial sediments (García-Meléndez et al., 2003).

At the limit between the Las Estancias range and the Huércal-Overa basin, the activity of the Alhama de Murcia fault led to the formation of a structural high, La Gata hills, which have blocked the alluvial fans draining the Las Estancias range. At some particular sites, the fluvial incision has permitted the drainage to overcome the structural barrier, giving rise to the formation of relatively younger alluvial fans at the toe of the La Gata hills (Fig. 1; Fig. 3; Table 1).

The El Límite fan has an elongated shape. Its western margin is particularly rectilinear. No faults have been observed along that margin, and the most probable cause of this geometry seems to be the draping of the fan onto the underlying alluvial fan surface, which is deformed by the activity of minor NE-SW faults oblique to the Alhama de Murcia fault system (Ortuño et al., 2012).

The age of this alluvial fan is especially interesting since it might correspond to a period of tectonic slow-down, in which the erosive capacity of the drainage could compete with the tectonic uplift of the La Gata hills. Additionally, alluvial fans generated in the same phase are folded and thrust by secondary faults of the Alhama de Murcia fault system (Ortuño et al., 2012). Thus, the dating of this alluvial phase is a clue in the determination of the fault slip-rates and the chronology of tectonic deformation.

El Límite fan is geomorphologically correlative with neighbouring fans that yielded an age of 50-125 ka (Ortuño et al., 2012), based on an improved

protocol for Infra-red stimulated luminescence (IRSL, see Sohbati et al., 2011, for details). These fans, including El Límite fan, belong to the third youngest alluvial fan generation of the Huércal-Overa basin (Table 2; Figs. 1 and 3).

3.1 Methods

Seven samples were collected from a road outcrop in El Lmite alluvial fan. Depths of amalgamated sediment samples were accurately controlled and measured by using a laser based device specifically designed for that purpose. Excepting LIM01, all samples were collected using a 5 cm diameter steel tube and a mallet. Owing to the fragility of the partially cemented fan material, the bulk density of the *in situ* sediment was measured in the field. Detachable sediment blocks of c. 1 kg wrapped with thin cellophane were weighed in atmosphere and water with a dinamometer. Bulk density was calculated by comparing both loads.

Quartz isolation was performed in the *Laboratori de Cosmonúclids Terrestres* of the *Universitat de Barcelona* (LCT-UB). Between 50 and 400 quartz pebbles (2-10 cm of diameter) from each sample were crushed and sieved to yield 250-1000 μm grains. The samples were then put through a Franz magnetic separator to remove any magnetic material. To eliminate carbonate, samples were digested in hydrochloric acid for 48 hours, using organic oil as an antifoam agent. After washing the oil residue, 3 hexafluorosilicic acid digestions were performed. Remaining quartz grains were cleaned using sequential hydrofluoric acid dissolutions to remove any potential atmospheric ^{10}Be (Brown et al., 1991; Kohl, 1992; Cerling, 1994). Between 15 to 20 g per sample of clean quartz cores were then dissolved in HF and spiked with ~ 200 mg of ^9Be carrier (Bourlès, 1988; Brown et al., 1992) at GU-SUERC Cosmogenic Isotope Laboratory.

Measurement of ^{10}Be and ^{26}Al concentrations was performed at the SUERC AMS facility at East-Kilbride (UK) in 2011 and 2012. All ^{10}Be and ^{26}Al concentrations are calibrated against the National Institute of Standards and Technology standard reference material 4325 by using an assigned value of $2.79 \cdot 10^{-11}$ $^{10}\text{Be}/^9\text{Be}$ and Z92-0222 standard with a nominal ratio of $4.11 \cdot 10^{-11}$ $^{26}\text{Al}/^{27}\text{Al}$.

^{10}Be and ^{26}Al concentrations in quartz were calculated following Balco (2006) (Table 2). Production rates and attenuation lengths were calculated using the CRONUS-earth online calculator v.2.2.1 MATLAB code from Balco

and Rovey (2008), modified to fit muon interaction cross-sections described in Braucher et al. (2013), Balco et al. (2013) and references therein. Thus, instead of the original values determined experimentally by Heisinger, we used the following values in the CRONUS Matlab code: $k_{neg10}=1.2916e-04$, $k_{neg26}=0.0016$, $\sigma_{190_10}=3.7822e-29$, $\sigma_{190_26}=6.9599e-28$. Calculated production rates and attenuation lengths are shown in table 1.

Apart from this, all the computations used the same constants as CRONUS-earth online calculators, explained in Balco et al. (2008), Balco (2009) and Balco (2010). Therefore, in all our calculations, a ^{10}Be decay constant of $4.9975 \cdot 10^{-7} \text{ a}^{-1}$ (Chmeleff et al., 2010), a ^{26}Al decay constant of $9.83 \cdot 10^{-7} \text{ a}^{-1}$ (Nishiizumi, 2004) and a spallation attenuation length of $\Lambda_{spall.} = 160 \text{ g cm}^{-2}$ (Balco et al., 2008) were used. The computation of ^{10}Be concentration models was performed using a computer algebra system software.

3.2 Data collection and results

A road outcrop across El Límite alluvial deposit was selected for depth profile sampling (Figs. 1 and 3; Tables 1 and 2). The outcrop is located c. 3 km south from the source area. In the sampling site area, the alluvial fan displays a continuous surface following the general alluvial fan slope, with no signs of erosion or incision. The alluvial deposit is mainly made up of light cemented gravel and conglomerate with a low matrix content (c. 65% pebbles, 10% sand, 5% silt, 5% carbonate cement). The high energy sedimentary facies are consistent with fast transportation. The fan surface has been used for farming, reworking the upper 20-40 cm of the deposit in the sampling site. This may be the origin of the outlier LIM01 ^{10}Be concentration. This sample also shows an outlier $^{26}\text{Al}/^{10}\text{Be}$ ratio, suggesting a different origin or analytical errors. Hence, LIM01 was not used in the models.

Most of the source area of these deposits is formed by Miocene (Lower Tortonian, c. 10 Ma, Voermans et al., 1974) conglomerate and Late Pleistocene alluvial fans (Fig. 1). As the age of the Miocene conglomerate is much longer than the half-life of the measured isotopes (1.387 and 0.705 Ma for ^{10}Be and ^{26}Al , respectively), they are not expected to conserve a significant inherited concentration of cosmogenic nuclides due to the exposure of the quartz grains prior to their burial in the Miocene. However, El Límite sediments are likely to have a certain concentration of ^{10}Be and ^{26}Al inherited from the exhumation, possible residence in older alluvial fans, and transportation during the Pleistocene.

The depositional matrix of the gravels is formed by fine sands and silts, presenting a limited and scattered nodular calcrete development as secondary cement. The density measurements yielded no significant difference between cemented and uncemented sediments, both with a mean density of $1.80 \pm 0.15 \text{ g cm}^{-3}$. This suggests diagenetic density variations lower than the density uncertainty and, hence, constant density models (Rodés et al., 2011) were used in the data analysis.

As the concentrations of the topmost sample were discarded, all models presented here have 4 free parameters fitting 12 data (6 ^{26}Al and 6 ^{10}Be measured concentrations), implying 8 degrees of freedom. To evaluate the benefits of the CSEB model *vs.* surface exposure model, both models were used. Model results are shown in Table 3 and Figs. 4 and 5.

4 Discussion

4.1 Model behaviour

The surface exposure model only provides a minimum age for the El Límite alluvial fan (Table 3), indicating that both ^{26}Al and ^{10}Be datasets are compatible with a saturated model ($t = \infty$). However, ^{26}Al and ^{10}Be apparent inheritances ($149 \pm 9 \cdot 10^3 \text{ }^{10}\text{Be}$ at g^{-1} and $948 \pm 64 \cdot 10^3 \text{ }^{26}\text{Al}$ at g^{-1}) shown in table 3 are only compatible with burial ages between 0 and 253 ka, according to Granger and Muzikar (2001) Fig. 1. A possible way to solve this inconsistency may be to iteratively reprocess the model limiting the possible values of t between 0 and the maximum age allowed by inheritance.

In contrast, the CSEB model directly provides consistent maximum and minimum ages (Table 3). As the maximum age is limited by the $^{26}\text{Al}/^{10}\text{Be}$ ratio of the modelled inheritance (Figs. 2 and 5), this model yields both maximum and minimum ages in datasets that trend to any significant ^{26}Al concentrations at great depths, i.e. datasets that indicate a significant amount of ^{10}Be and ^{26}Al apparent current inheritance. As maximum ages of the results obtained using the CSEB model depend on the current $^{26}\text{Al}/^{10}\text{Be}$ ratio of the apparent inheritance rather than in the absolute ^{26}Al and ^{10}Be concentrations, the maximum ages obtained with the CSEB model are expected to be less sensitive to muon production rates than the ones obtained with the exposure model.

4.2 El Límite Alluvial Fan

Table 3 shows minimum χ^2 values between 8 and 9. Considering that all models have 8 degrees of freedom, this values imply minimum reduced χ^2 values of ~ 1 , suggesting that uncertainties of the input data (concentration, depth and density) roughly reflect the effects of natural processes not considered in the models.

We would like to emphasize that results shown in table 3 are obtained only from the theoretical models fitting the El Límite ^{10}Be - ^{26}Al dataset, for model testing purposes. No geological constraint was imposed. This means that, by considering a different dataset, restricting the models from geological evidence or multiple depth-profile datasets, the deduced deposition age may be better constrained. If a maximum erosion rate of El Límite fan surface can be determined by independent evidence, the deducted deposition age will be in the low range of the ages shown in table 3 (e.g. Rodés et al., 2011). Also, if a set of depth-profiles are sampled in different alluvial deposits with a clear relative chronology (e.g. fluvial terrace series), the superposition of resulting age distribution will allow to constrain each individual age.

Age results from El Límite ^{10}Be and ^{26}Al dataset (11-213 ka) are in good agreement with independent IRSL ages obtained in the same unit by Ortuño et al. (2012) (Late Pleistocene). The CSEB model also suggest that sediments forming El Límite alluvial fan were exhumed from the source area in the Late Pleistocene, Middle Pleistocene or before ($t_b + t \sim 11 - 220$ ka; Fig. 5). As we cannot assume a continuous deep shielding of the sediments between exhumation and deposition in El Límite, we must consider $t + t_b$ as a minimum exhumation age of El Límite sediments. Therefore, according to Ortuño et al. (2012) data and the CSEB model results, this alluvial fan is the result of the reworking of older alluvial deposits, revealing a complex transportation history from the source area (Pliocene conglomerate) to El Límite alluvial fan. Fig 1 shows that older and deformed alluvial sediments (Middle Pleistocene; Ortuño et al., 2012) are located at both sides of the South Alhama de Murcia fault, surrounding the apex of El Límite alluvial fan. All these results support that the origin of the El Límite alluvial fan is related with the tectonic growth and the subsequent erosion of the Góñar anticline, a compressive bend formed between the South and the North Alhama de Murcia faults (the La Gata hills are part of the southern flank of this anticline, preserved from the erosion). The source area of the fan is therefore not the Las Estancias range.

Apparent exhumation rates of the CSEB model results yield values of

30 – 40 mm ka⁻¹. According to Fig. 2, apparent exhumation rate represents a minimum value for the mean exhumation rate in the sediment-source area at the moment these sediments were generated. Despite the fact that exhumation is a process occurring at a basin scale and we are assuming an equilibrium steady state, the original sediment-source area of El Límite fan represents a small area compared to the area affected by the Alhama de Murcia fault system. Therefore, we consider that the calculated apparent exhumation rate for the source area of El Límite sediments must be interpreted as a minimum value for a process that is strongly restricted in time and space. Nevertheless, the minimum 32 – 38 mm ka⁻¹ exhumation rate is in excellent agreement with individual vertical slip rates of Alhama de Murcia-Goñar fault system calculated by independent methods (10-80 mm ka⁻¹; Ortuño et al., 2012).

5 Conclusions

The combined surface exposure-burial (CSEB) model allow to calculate minimum and maximum ages of deposits using paired cosmogenic nuclide datasets, providing a robust maximum age even with datasets that seem saturated using a surface exposure model.

Combination of Monte-Carlo and χ^2 minimization approaches avoids the need to enter an approximated solution or to constrain parameter values before the model fitting. This allows to get fast and independent results when fitting the models.

The CSEB model can be used, not only to date a landform, but also to provide data related to the sedimentological history prior to deposition. ε_r and t_b parameters provide minimum constraints to the exhumation rate and sediment residence time, respectively. These constraints are highly valuable for the paleoclimate and paleotectonic studies of Quaternary basins.

Models fitting El Límite dataset suggest that this alluvial fan is formed by reworked alluvial sediments that were redeposited in the Late Pleistocene, probably related to the South Alhama de Murcia fault activity. Also, model results suggest vertical slip rates of the Alhama de Murcia fault system of about 36 mm ka⁻¹ or greater.

6 Acknowledgements

We thank Lena Driehaus (UB), M^a José Aguilar Perez (UB) and María Miguens-Rodriguez (GU-SUERC) for their help in the lab, and Sheng Xu for ^{10}Be and ^{26}Al AMS measurements. This work was founded by the Spanish Ministerio de Educación y Ciencia through the EVENT (CGL2006-12861-C02-01/BTE) and the SHAKE (CGL2011-30005-C02-01/BTE) projects and the Consolider-Ingenio 2010 programme, under CSD2006-0004 “Topo-Iberia”.

7 Tables

Location	Latitude (N)	Longitude (W)	Elevation (m)
Sampling site	37.484830	1.865754	448
Source area	37.5	1.9	600

Location	Isotope	$P_{spal.}$ (atoms $g^{-1}a^{-1}$)	P_{stop} (atoms $g^{-1}a^{-1}$)	P_{fast} (atoms $g^{-1}a^{-1}$)	$\Lambda_{spal.}$ ($g \cdot cm^{-2}$)	Λ_{stop} ($g \cdot cm^{-2}$)	Λ_{fast} ($g \cdot cm^{-2}$)
Sampling site	^{10}Be	5.8505	0.0296	0.0410	160	1137	1842
Sampling site	^{26}Al	39.4713	0.3731	0.3769	160	1137	1842
Source area	^{10}Be	6.6216	0.0316	0.0423	160	1057	1772
Source area	^{26}Al	44.6730	0.3987	0.3895	160	1057	1772

Table 1: Location of El Límite sampling site and El Puntal source area in Las Estancias Range (mean altitude), and ^{10}Be and ^{26}Al production rates (P) and attenuation lengths (Λ) of spallation, stopping muons and fast muons cross sections according to Balco et al. (2008) and Balco et al. (2013).

Sample	Depth (cm)	^{10}Be AMS ID	^{10}Be concentration ($at \cdot g^{-1}$)	^{26}Al AMS ID	^{26}Al concentration ($at \cdot g^{-1}$)
LIM01	5 ± 5	b5070	162134 ± 4076	a1442	1427800 ± 60059
LIM02	25 ± 3	b5073	208193 ± 6099	a1445	1345488 ± 67228
LIM03	50 ± 3	b5074	199409 ± 5066	a1446	1280169 ± 59487
LIM04	80 ± 3	b5075	201078 ± 5724	a1447	1195957 ± 71935
LIM05	130 ± 3	b5076	173624 ± 5150	a1448	1133691 ± 59485
LIM06	180 ± 3	b5077	165973 ± 5102	a1449	1128188 ± 60445
LIM07	260 ± 3	b5079	153708 ± 5323	a1451	967850 ± 62394

Table 2: The El Límite sample depths and ^{10}Be and ^{26}Al concentrations. The values of the blank samples yielded $5 \cdot 10^{-15}$ atoms of $^{10}Be/Be$ and $8 \cdot 10^{-16}$ atoms of $^{26}Al/Al$. Concentration uncertainties include the blank concentration uncertainty, measurement error and spectrometer standard error.

Model	Results	χ^2	Inheritance ^{10}Be (10^3 at g^{-1})	Inheritance ^{26}Al (10^3 at g^{-1})	ε_r (mm ka^{-1})	t_b (ka)	ε (mm ka^{-1})	t (ka)
Exposure	χ^2_{min}	8.5	149	948			68	∞
Exposure	χ^2_{max}	12.7	142 – 159	882 – 1010			0 – 90	11 – ∞
CSEB	χ^2_{min}	8.8			36	0	66	76
CSEB	χ^2_{max}	12.9			32 – 38	0 – 191	0 – 89	11 – 213

Table 3: Surface exposure and CSEB models results ($\nu = 12$ data - 4 parameters = 8 degrees of freedom). χ^2_{min} is the total minimum value of the χ^2 function that is reached at the best fit. χ^2_{max0} is the maximum χ^2 value fitting the data within one σ confidence level (see Rodés et al., 2011). Probability distributions of inheritance and ε_r are similar to Gaussian distribution. Probability distributions of t_b are similar to a Gaussian distribution centered in 0 ka. Probability distributions of t are between Gamma-like and uniform distributions.

8 Figure captions

Fig. 1: Location of ^{10}Be - ^{26}Al depth profile (star) in the El Límite alluvial fan. The sampling area is located on the SE slope of Las Estancias antiform, bounded by Quaternary basin sediments that fill the eastern Huércal-Overa basin (eastern Betic Cordillera, SE Spain), and affected by the Quaternary activity of the left-lateral, reverse Alhama de Murcia fault, composed of two NE-SW strands: the Northern Alhama de Murcia Fault (North AMF) and the Southern Alhama de Murcia Fault (South AMF). Ortuño et al. (2012) studied alluvial fan formation phases using IRSL dating, yielding ages from Middle Pleistocene (phase 5) to present.

Fig. 2: Example of cosmogenic signature evolution of sediments in a 2-isotope banana plot (Bierman et al., 1999) using hypothetical data. Concentrations are scaled to their surface production rates. Both constant-exposure and erosion-equilibrium are represented by thick lines. Exhumation rates are indicated along erosion-equilibrium line. Gray lines represent the apparent burial ages according to burial model (Eq. 5). The example evolution of ^{10}Be - ^{26}Al starts with rock exhumation at the sediment-source area at a rate of 100 m/Ma (1-2). After a complex history of more than 0.3 Ma including several burial (2-3, 4-5, 6-7) and exposure (3-4, 5-6) phases, the sediments are exposed forming an alluvial deposit (7) and the final cosmogenic signatures evolve as function of the depth below the surface (7 to squares). The CSEB model allows to calculate the cosmogenic signature of point 7 by inverse approach. Apparent exhumation rate (ε_r ; projection of point 7 over erosion-equilibrium line), apparent residence time (t_b ; from point 7 to erosion-equilibrium line) and exposure age (t ; from apparent current inheritance to point 7) of the example model are 30 m/Ma, 0.2 Ma and 0.2 Ma respectively.

Fig. 3: Road-cut outcrop excavated across the El Límite alluvial fan, where a 3 m deep depth profile was sampled.

Fig. 4: ^{10}Be and ^{26}Al sample concentrations vs. depth. Error bars include concentration and depth uncertainties. Best fit of the ^{10}Be - ^{26}Al CSEB model is depicted by black thick lines. ^{10}Be - ^{26}Al CSEB models that fit the measured ^{10}Be - ^{26}Al dataset within 1σ confidence level are depicted by gray areas. Both exposure and CSEB model results show similar best fit profiles.

Fig. 5: Projection of the ε_r - t_b - ε - t hyper-volumes corresponding to CSEB model results that fit the data within 5%, 10%, 20%, 40% and 1σ confidence level. Gray lines show equal $t+t_b$. As suggested in Fig. 2, the CSEB model

fits yield quasi-constant $t+t_b$ results, mostly depending on the apparent current ^{10}Be - ^{26}Al inheritance.

Figure 1: Rodés et al.

Figure 2: Rodés et al.

Figure 3: Rodés et al.

Figure 4: Rodés et al.

ACCEPTED MANUSCRIPT

Figure 5: Rodés et al.

ACCEPTED MANUSCRIPT

References

- Anderson, R. S., Repka, J. L., Dick, G. S., 1996. Explicit treatment of inheritance in dating depositional surfaces using in situ ^{10}Be and ^{26}Al . *Geology* 24 (1), 47–51.
- Balco, G., 2006. Converting Al and Be isotope ratio measurements to nuclide concentrations in quartz. Cosmogenic Nuclide Lab, University of Washington, <http://hess.ess.washington.edu>.
- Balco, G., 2009. ^{26}Al - ^{10}Be exposure age/erosion rate calculators: update from v. 2.1 to v. 2.2. Cosmogenic Nuclide Lab, University of Washington, <http://hess.ess.washington.edu>.
- Balco, G., 2010. ^{26}Al - ^{10}Be exposure age/erosion rate calculators: update of constants file from 2.2 to 2.2.1. Cosmogenic Nuclide Lab, University of Washington, <http://hess.ess.washington.edu>.
- Balco, G., Purvance, M. D., Rood, D. H., 2011. Exposure dating of precariously balanced rocks. *Quaternary Geochronology* 6 (34), 295 – 303.
- Balco, G., Rovey, C. W., 2008. An isochron method for cosmogenic-nuclide dating of buried soils and sediments. *American Journal of Science* 308 (10), 1083–1114.
- Balco, G., Soreghan, G. S., Sweet, D. E., Marra, K. R., Bierman, P. R., 2013. Cosmogenic-nuclide burial ages for Pleistocene sedimentary ll in Unaweep Canyon, Colorado, USA. *Quaternary Geochronology* (in press), <http://dx.doi.org/10.1016/j.quageo.2013.02.002>.
- Balco, G., Stone, J. O., Lifton, N. A., Dunai, T. J., 2008. A complete and easily accessible means of calculating surface exposure ages or erosion rates from ^{10}Be and ^{26}Al measurements. *Quaternary Geochronology* 3 (3), 174 – 195.
- Bierman, P. R., Marsella, K. A., Patterson, C., Davis, P., Caffee, M., 1999. Mid-Pleistocene cosmogenic minimum-age limits for pre-Wisconsinan glacial surfaces in southwestern Minnesota and southern Baffin Island: a multiple nuclide approach. *Geomorphology* 27 (12), 25 – 39.

- Bourlès, D. L., 1988. Etude de la géochimie de l'isotope cosmogénique ^{10}Be et de son isotope stable ^9Be en milieu océanique. Application à la datation des sédiments marins. Ph.D. thesis, Paris-sud, Centre d'Orsay.
- Braucher, R., Bourlès, D., Merchel, S., Romani, J. V., Fernandez-Mosquera, D., Marti, K., Lanni, L., Chauvet, F., Arnold, M., Aumatre, G., Keddadouche, K., 2013. Determination of muon attenuation lengths in depth profiles from in situ produced cosmogenic nuclides. *Nuclear Instruments and Methods in Physics Research Section B: Beam Interactions with Materials and Atoms* 294 (0), 484 – 490, Proceedings of the Twelfth International Conference on Accelerator Mass Spectrometry, Wellington, New Zealand, 20-25 March 2011.
- Braucher, R., Castillo, P. D., Siame, L., Hidy, A., Bourlès, D., 2009. Determination of both exposure time and denudation rate from an in situ-produced ^{10}Be depth profile: A mathematical proof of uniqueness. Model sensitivity and applications to natural cases. *Quaternary Geochronology* 4 (1), 56 – 67.
- Braucher, R., Merchel, S., Borgomano, J., Bourlès, D., 2011. Production of cosmogenic radionuclides at great depth: A multi element approach. *Earth and Planetary Science Letters* 309 (12), 1 – 9.
- Brown, E. T., Brook, E. J., Raisbeck, G. M., Yiou, F., Kurz, M. D., 1992. Effective attenuation lengths of cosmic rays producing ^{10}Be and ^{26}Al in quartz: implications for exposure age dating. *Geophysical Research Letters* 19 (4), 369–372.
- Brown, E. T., Edmond, J. M., Raisbeck, G. M., Yiou, F., Kurz, M. D., Brook, E. J., 1991. Examination of surface exposure ages of Antarctic moraines using in situ produced ^{10}Be and ^{26}Al . *Geochimica et Cosmochimica Acta* 55 (8), 2269 – 2283.
- Cerling, T.E., C. H., 1994. Geomorphology and in-situ cosmogenic isotopes. *Annual Review of Earth & Planetary Sciences* 22, 273–317.
- Chmeleff, J., von Blanckenburg, F., Kossert, K., Jakob, D., 2010. Determination of the ^{10}Be half-life by multicollector ICP-MS and liquid scintillation counting. *Nuclear Instruments and Methods in Physics Research Section B: Beam Interactions with Materials and Atoms* 268 (2), 192 – 199.

- García-Meléndez, E., Goy, J., Zazo, C., 2003. Neotectonics and Plio-Quaternary landscape development within the eastern Huércal-Overa Basin (Betic Cordilleras, southeast Spain). *Geomorphology* 50 (13), 111 – 133.
- Gosse, J. C., Phillips, F. M., 2001. Terrestrial in situ cosmogenic nuclides: theory and application. *Quaternary Science Reviews* 20 (14), 1475 – 1560.
- Granger, D. E., Muzikar, P. F., 2001. Dating sediment burial with in situ-produced cosmogenic nuclides: theory, techniques, and limitations. *Earth and Planetary Science Letters* 188 (1-2), 269–281.
- Granger, D. E., Smith, A. L., 2000. Dating buried sediments using radioactive decay and muogenic production of ^{26}Al and ^{10}Be . *Nuclear Instruments and Methods in Physics Research Section B: Beam Interactions with Materials and Atoms* 172 (14), 822 – 826.
- Hancock, G. S., Anderson, R. S., Chadwick, O. A., Finkel, R. C., 1999. Dating fluvial terraces with ^{10}Be and ^{26}Al profiles: application to the Wind River, Wyoming. *Geomorphology* 27 (12), 41 – 60.
- Heisinger, B., Lal, D., Jull, A., Kubik, P., Ivy-Ochs, S., Knie, K., Nolte, E., 2002a. Production of selected cosmogenic radionuclides by muons: 2. Capture of negative muons. *Earth and Planetary Science Letters* 200 (34), 357 – 369.
- Heisinger, B., Lal, D., Jull, A., Kubik, P., Ivy-Ochs, S., Neumaier, S., Knie, K., Lazarev, V., Nolte, E., 2002b. Production of selected cosmogenic radionuclides by muons: 1. Fast muons. *Earth and Planetary Science Letters* 200 (34), 345 – 355.
- Hidy, A. J., Gosse, J. C., Pederson, J. L., Mattern, J. P., Finkel, R. C., 2010. A geologically constrained Monte Carlo approach to modeling exposure ages from profiles of cosmogenic nuclides: An example from Lees Ferry, Arizona. *Geochemistry Geophysics Geosystems* 11 (September), doi:10.1029/2010GC003084.
- Kohl, C.P., N. K., 1992. Chemical isolation of quartz for measurement of in-situ -produced cosmogenic nuclides. *Geochimica et Cosmochimica Acta* 56 (9), 3583–3587.

- Lal, D., 1991. Cosmic ray labeling of erosion surfaces: in situ nuclide production rates and erosion models. *Earth and Planetary Science Letters* 104 (2-4), 424 – 439.
- Mercader, J., Gosse, J. C., Bennett, T., Hidy, A. J., Rood, D. H., 2012. Cosmogenic nuclide age constraints on Middle Stone Age lithics from Niassa, Mozambique. *Quaternary Science Reviews* 47 (0), 116 – 130.
- Nishiizumi, K., 2004. Preparation of ^{26}Al AMS standards. In: *Proceedings of the Ninth International Conference on Accelerator Mass Spectrometry*. Vol. 223 - 224. pp. 388 – 392.
- Nissen, E., Walker, R. T., Bayasgalan, A., Carter, A., Fattahi, M., Molor, E., Schnabel, C., West, A. J., Xu, S., 2009. The late Quaternary slip-rate of the Har-Us-Nuur fault (Mongolian Altai) from cosmogenic ^{10}Be and luminescence dating. *Earth and Planetary Science Letters* 286 (34), 467 – 478.
- Ortuño, M., Masana, E., García-Meléndez, E., Martínez-Díaz, J., Štěpančiková, P., Cunha, P. P., Sohbati, R., Canora, C., Buylaert, J.-P., Murray, A. S., 2012. An exceptionally long paleoseismic record of a slow-moving fault: the Alhama de Murcia fault (Eastern Betic Shear Zone, Spain). *The Geological Society of America Bulletin* (in press).
- Rodés, A., Pallàs, R., Braucher, R., Moreno, X., Masana, E., Bourles, D. L., 2011. Effect of density uncertainties in cosmogenic ^{10}Be depth-profiles: Dating a cemented Pleistocene alluvial fan (Carboneras Fault, SE Iberia). *Quaternary Geochronology* 6 (2), 186 – 194.
- Siame, L., Bellier, O., Braucher, R., Sbrier, M., Cushing, M., Bourles, D., Hamelin, B., Baroux, E., de Voogd, B., Raisbeck, G., Yiou, F., 2004. Local erosion rates versus active tectonics: cosmic ray exposure modelling in Provence (south-east France). *Earth and Planetary Science Letters* 220 (34), 345 – 364.
- Sohbati, R., Murray, A. S., Buylaert, J.-P., Ortuño, M., Cunha, P. P., Masana, E., 2011. Luminescence dating of Pleistocene alluvial sediments affected by the Alhama de Murcia fault (eastern Betics, Spain) a comparison between OSL, IRSL and post-IRIRSL ages. *Boreas*, 10.1111/j.1502-3885.2011.00230.x.

Voermans, F., Simón, O., Martín-García, L., Gómez-Prieto, J., 1974. Mapa geológico de España, Huercal-Overa, hoja 996. Ministerio de Industria y Energía, Madrid.

Wolkowinsky, A. J., Granger, D. E., 2004. Early Pleistocene incision of the San Juan River, Utah, dated with ^{26}Al and ^{10}Be . *Geology* 32 (9), 749–752.

1°53'0"W

1°52'0"W

1°51'0"W

Legend

-  Reverse fault
-  Antiform
-  Synform
-  Major fault
-  Inferred major fault
-  Inferred minor fault

Quaternary units

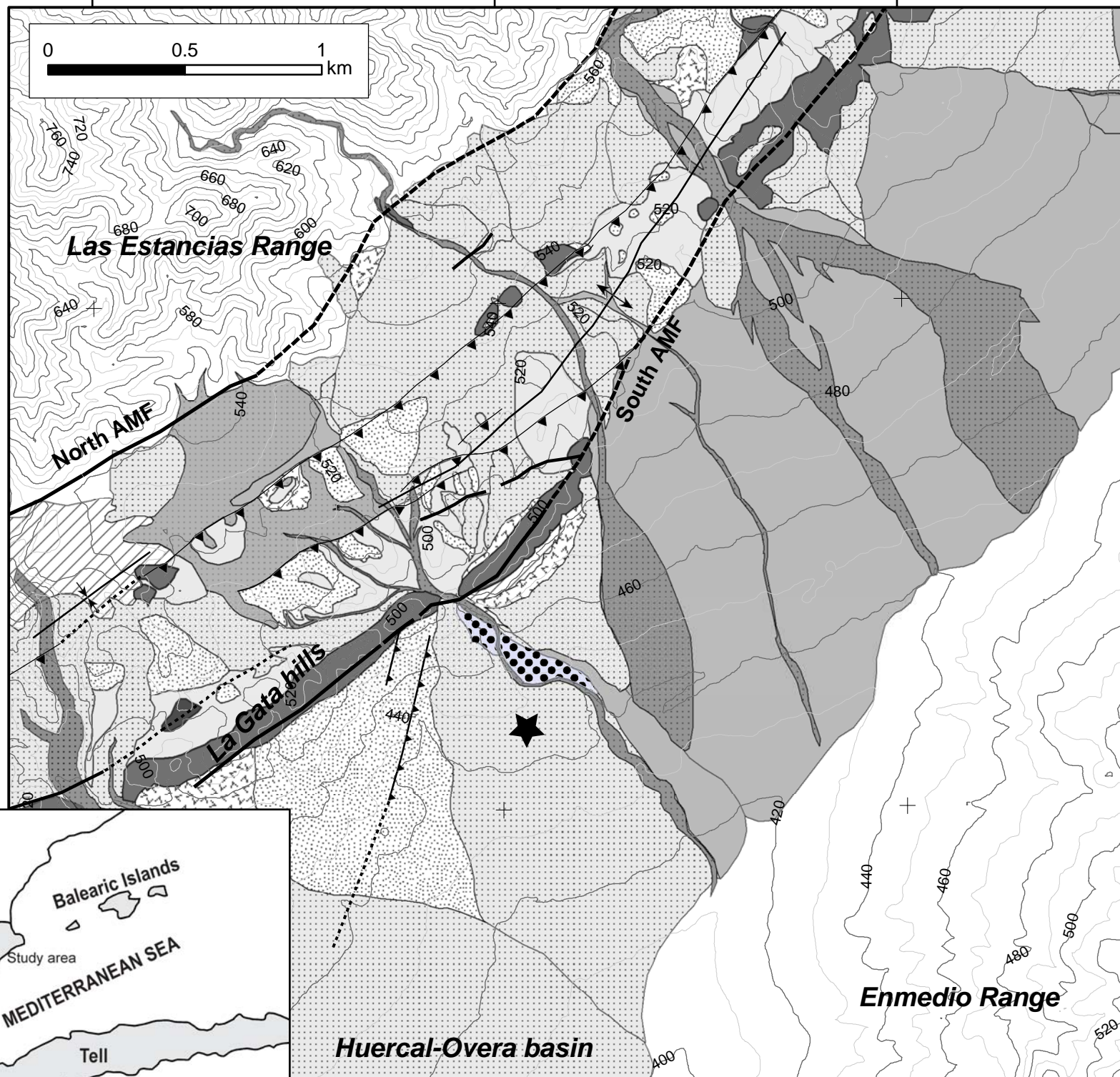
-  Slope debris
-  Alluvial terrace

Alluvial fans

-  Active phase (1)
-  Phase 2
-  Phase 3
-  Phase 4
-  Phase 5

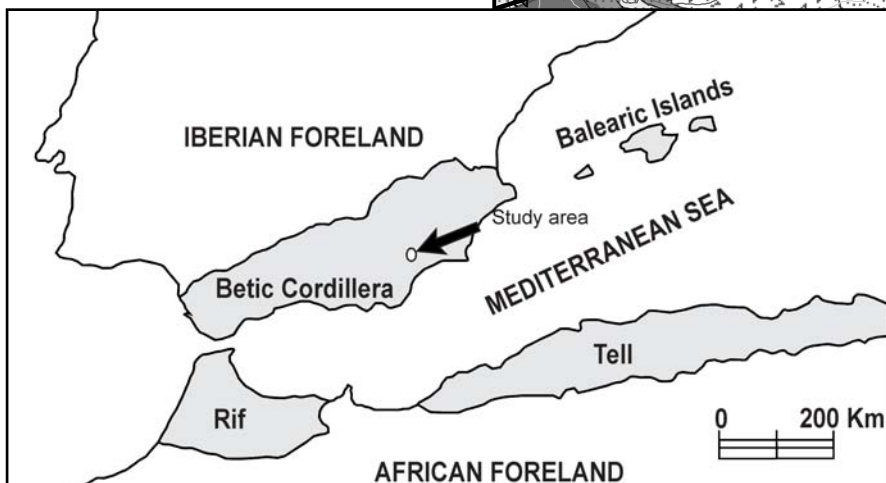
Pre-Quaternary units

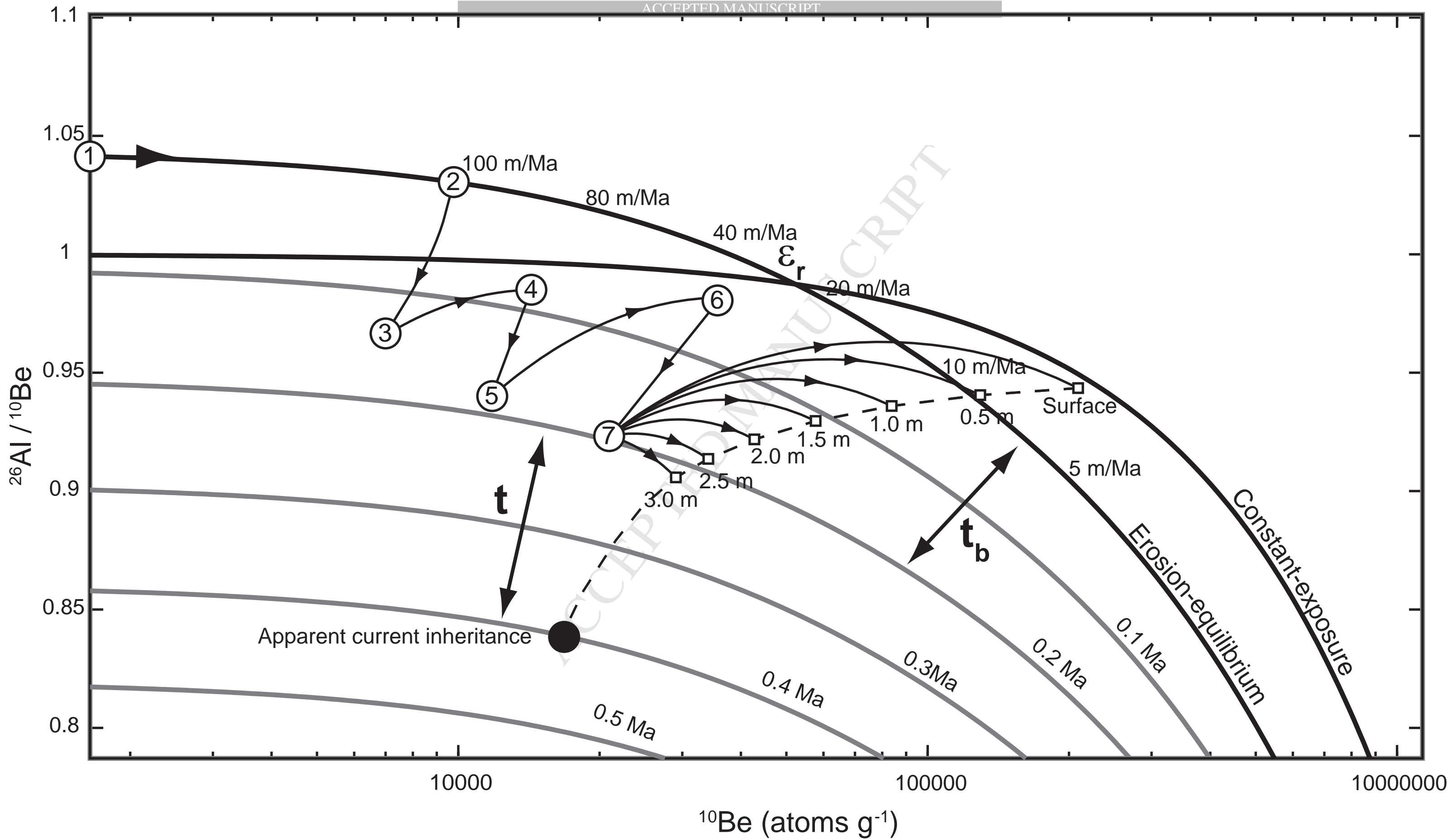
-  Miocene/Pliocene Conglomerate
-  Miocene Marls/Conglomerate
-  Basement



37°30'0"N

37°29'0"N





La Gata Hills

Las Estancias Range

El Límite fan



